Japanese Journal of Applied Physics **57**, 018001 (2018)
https://doi.org/10.7567/JJAP.57.018001

BRIEF NOTE

Long-term stability enhancement of Brillouin measurement in polymer optical fibers using amorphous fluoropolymer

Natsuki Matsutani, Heeyoung Lee, Yosuke Mizuno*, and Kentaro Nakamura

Institute of Innovative Research, Tokyo Institute of Technology, Yokohama 226-8503, Japan

*E-mail: ymizuno@sonic.pi.titech.ac.jp

Received October 3, 2017; accepted November 21, 2017; published online December 13, 2017

For Brillouin-sensing applications, we develop a method for mitigating the Fresnel reflection at the perfluorinated-polymer-optical-fiber ends by covering them with an amorphous fluoropolymer (CYTOP, fiber core material) dissolved in a volatile solvent. Unlike the conventional method using water, even after solvent evaporation, the CYTOP layer remains, resulting in long-term Fresnel reduction. In addition, the high viscosity of the CYTOP solution is a practical advantage. The effectiveness of this method is experimentally proved by Brillouin measurement.

Brillouin scattering in optical fibers has drawn significant attention in the sensing community as it can be exploited to measure the strain and temperature distributions.[1–18] In 2010, Brillouin scattering in polymer optical fibers (POFs) was observed for the first time;[19] since then, several research groups have been developing POF-based Brillouin sensors[20–23] with large-strain measurability,[24] greater ease of handling, and the so-called memory functions of strain[25] and temperature.[26] Unlike the other groups studying POF-based Brillouin sensing with two-end-access configurations (Brillouin optical time-domain analysis[20] and Brillouin optical frequency-domain analysis[21]), we have been in the process of developing POF-based single-end-access distributed sensing systems, using a unique technique called Brillouin optical correlation-domain reflectometry (BOCDR).[17,18] In addition to the single-end accessibility, the advantages of BOCDR include high spatial resolution, random accessibility, and cost efficiency. Recently, several high-speed BOCDR configurations were implemented[27–29] and successfully applied to POF-based sensing.[23]

Various types of POFs have been developed in addition.[30–33] For instance, the most common POF composed of polymethyl methacrylate is optimized for visible light transmission; however, its propagation loss at telecom wavelength is considerably high ($\gg$100 dB/m), rendering it unsuitable for Brillouin applications.[30] The only type in which Brillouin scattering has been experimentally observed is the perfluorinated graded-index (PFGI-) POF,[19,31] with relatively low propagation loss, even at telecom wavelength.

In BOCDR using PFGI-POF (core refractive index, $n \simeq 1.36$) as the fiber under test (FUT), when the Fresnel reflections at both ends of the PFGI-POF, i.e., the boundary with a silica single-mode fiber (SMF; $n \simeq 1.46$) and that with air ($n \simeq 1.00$), are significant, the Brillouin gain spectrum (BGS) is overlapped with interference noise in general.[34] It is temporally unstable, and the measurement accuracy of the Brillouin frequency shift (BFS), which provides the information on strain and temperature, deteriorates for high-speed configurations in particular.[27–29]

When the FUT is a silica SMF, in addition to the weak Fresnel reflection at the proximal end, the Fresnel reflection at the distal open end of the FUT can also be sufficiently reduced by applying considerable bending loss near the end or by cutting the end with an angle. However, when the FUT is PFGI-POF, it is difficult to apply sufficient bending loss near the open end of the FUT, because PFGI-POF is a multimode fiber with a core diameter of at least 50 μm and is nearly insusceptible to bending loss.[31] To employ an angled-cut end is one method of suppressing the Fresnel reflection, but it is not constantly effective for a multimode fiber. Therefore, the Fresnel reflection at the open end of the PFGI-POF has conventionally been suppressed by immersing the end in water, which has a refractive index ($n \simeq 1.33$) close to that of the PFGI-POF core. However, when the tip of the PFGI-POF is removed from water, a high-power light is radiated at the open end and the water evaporates rapidly; thus, it is not easy to use this method for long-term measurement.

In this work, we develop a new method for mitigating the Fresnel reflection at the open end of the PFGI-POF by covering the end with an amorphous fluoropolymer (cyclic transparent optical polymer, Asahi Glass CYTOP®), which constitutes the same material as that of the PFGI-POF core, dissolved in a volatile solvent. Even after the solvent evaporates, the CYTOP layer remains attached to the open end, resulting in long-term Fresnel reduction. In addition, as the core and CYTOP material are the same, the refractive index matching can be more ideal than in the case of water. We experimentally demonstrate the effectiveness of this method using Brillouin measurement.

A 2.6-m-long PFGI-POF was employed as the FUT. It consists of a core (50 μm diameter) with cladding (100 μm diameter) and overcladding (750 μm diameter). The core and cladding layers are composed of doped and undoped CYTOP, respectively. The refractive index at the center of the core is 1.356 and that of the cladding layer is 1.342;[35] these values are not strongly dependent on the optical wavelength.[36] The propagation loss at 1.55 μm is ~0.25 dB/m.

The experimental setup for measuring the temporal variations in the Fresnel-reflected light power, before and after covering the open end of the PFGI-POF with water and CYTOP solution, respectively, is depicted in Fig. 1. The output of a semiconductor laser at 1.55 μm was injected into one end of the PFGI-POF via an optical circulator (OC) composed of silica SMFs. The incident power was maintained at 23.5 dBm by using an erbium-doped fiber amplifier. The polarization state was scrambled to suppress the polarization-dependent signal fluctuations. The SMF, which is the second port of the OC, was butt-coupled to the PFGI-POF;[19] this part was fixed during all measurements, which resulted in a constant Fresnel reflection. Consequently, the power change was attributed to the Fresnel reflection at the other end of the PFGI-POF. With a photo detector (PD), the reflected light

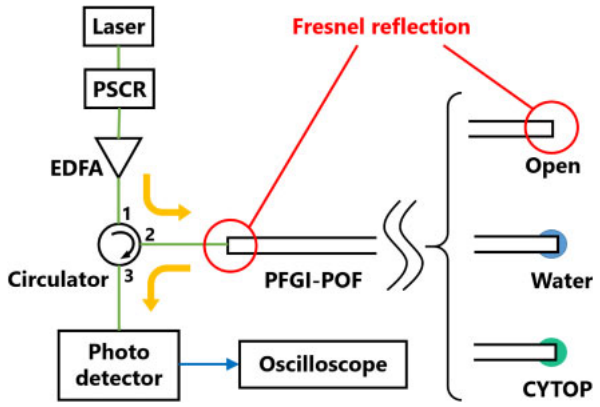

Fig. 1. (Color online) Experimental setup. EDFA: erbium-doped fiber amplifier; PFGI-POF: perfluorinated graded-index polymer optical fiber; PSCR: polarization scrambler.

was converted into an electrical signal, which was observed using an oscilloscope in real-time. The tip of the PFGI-POF, which was perpendicularly cut and polished, was entirely immersed in water or CYTOP solution [CTX-809SP2; concentration: 9%; solvent: CT-SOLV180 ($n \simeq 1.29$)] and was subsequently removed. Note that the simply calculated reflectivities at the PFGI-POF end covered with air, water, and CYTOP solution (before solvent evaporation) are approximately 2.2, 0.006, and 0.03%, respectively. Moreover, BGS measurement was performed using the setup shown in Fig. 1 by replacing the PD with an electrical spectrum analyzer. In this configuration, without using an explicit reference light path, the Fresnel-reflected light operates as the reference light for BGS detection.[37)]

The temporal variations in the Fresnel-reflected light power, before immersing the open end of the PFGI-POF in water, while immersed in water, and shortly (1 min) after removing from water are depicted in Figs. 2(a), 2(b), and 2(c), respectively. The vertical axis was normalized to make the average power in Fig. 2(a) (−54.2 dBm), 0 dB. In this figure, the Fresnel reflection at the open end was temporally unstable with a standard deviation (SD) of ±1.67 dB. Then, when the open end was immersed in water, the temporal signal fluctuations were suppressed to an SD of ±0.94 dB owing to refractive index matching. However, 1 min after removing the PFGI-POF from water, the signal fluctuations increased to almost the same value as those before immersion, with an SD of ±1.29 dB. This is because the remaining water on the core evaporated rapidly owing to high-power light radiation and the index matching was no longer valid. Thus, covering the PFGI-POF end with water was demonstrated to be unsuitable for reducing Fresnel reflection.

Subsequently, similar measurements were performed using CYTOP solution. The temporal variations in the Fresnel-reflected light power before immersing the open end of the PFGI-POF in the CYTOP solution, while submerged in the solution, and 1 min and 24 h after removal from the solution are shown in Figs. 3(a), 3(b), 3(c), and 3(d), respectively. In Fig. 3(a), the signal fluctuations are relatively large with an SD of ±1.64 dB, comparable to that in Fig. 2(a) as the measurement condition is similar. When the open end was immersed in the CYTOP solution for refractive index matching, the signal fluctuations were suppressed to an SD of ±0.52 dB, as in water. Then, 1 min after removing the PFGI-

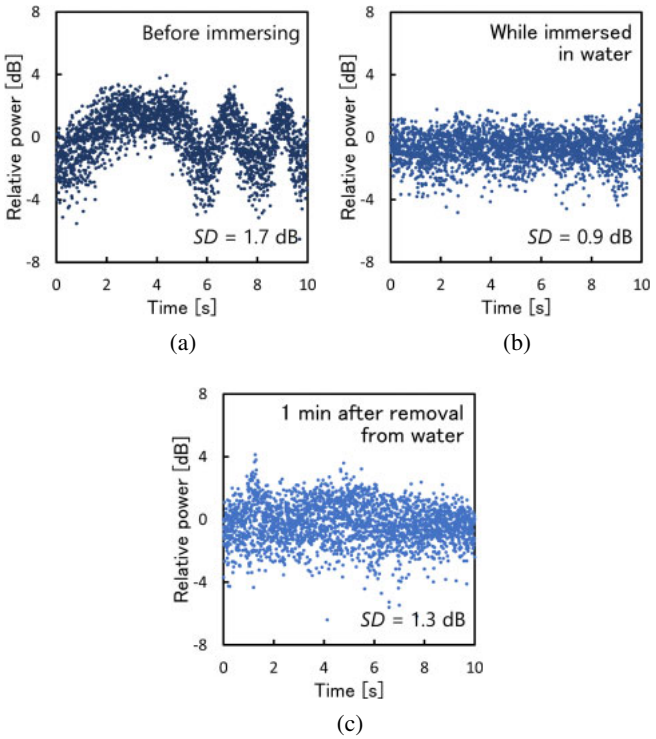

Fig. 2. (Color online) Temporal variations in the Fresnel-reflected light power (a) before immersing the open end of the PFGI-POF in water, (b) while immersed in water, and (c) 1 min after removal from water. The SDs of the signal fluctuations are indicated.

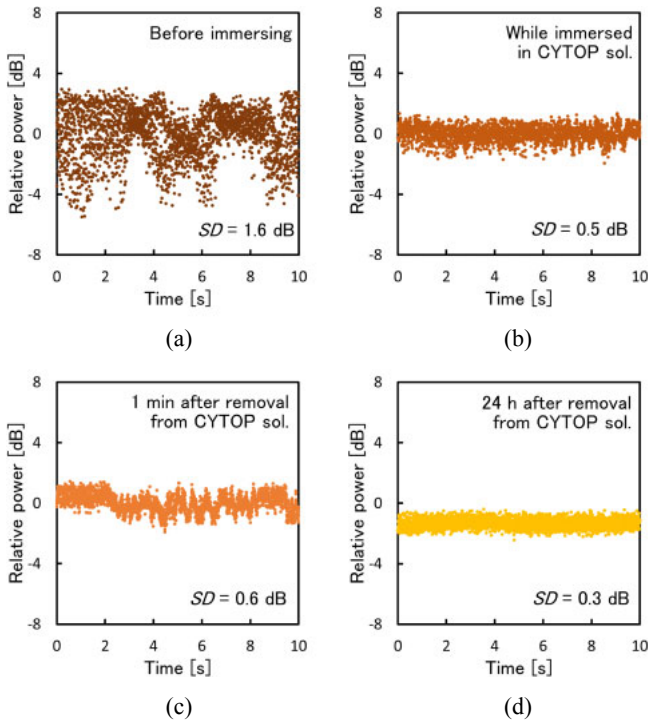

Fig. 3. (Color online) Temporal variations in the Fresnel-reflected light power (a) before immersing the open end of the PFGI-POF in CYTOP solution, (b) while immersed, and (c) 1 min and (d) 24 h after removal from the CYTOP solution. The SDs of the signal fluctuations are indicated.

POF end from the CYTOP solution, the suppression of the signal fluctuation continued to an SD of ±0.58 dB, due to the high viscosity of the solution. Moreover, 24 h after removal from the CYTOP solution, the signal fluctuations were

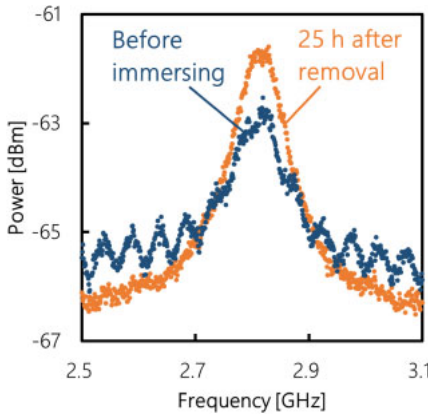

Fig. 4. (Color online) BGSs measured before immersing the PFGI-POF end in CYTOP solution (blue) and 25 h after removal (orange).

suppressed further to an SD of ±0.33 dB. Unlike the case of water, after solvent evaporation, the CYTOP solidified and remained on the core. The enhanced suppression of the signal fluctuations was probably caused by the more ideal refractive index matching between the PFGI-POF core ($n \simeq 1.36$) and the CYTOP ($n \simeq 1.35$) (note that the refractive index of the CYTOP solution is lower than ∼1.35, because the refractive index of its solvent is ∼1.29). Thus, covering the PFGI-POF end with high-viscosity CYTOP solution was demonstrated to be suitable for long-term Fresnel reduction.

Finally, we measured the BGSs of the same PFGI-POF, before immersing its open end in CYTOP solution and 25 h after removal, as shown in Fig. 4. Before immersing, the BGS was overlapped with the interference noise caused by the multiple Fresnel reflections at both the ends of the PFGI-POF. The peak interval of the noise was approximately 40 MHz, which corresponds well with the theoretical value calculated using the PFGI-POF length.[34)] However, it is evident that the noise was reduced by CYTOP usage, resulting in an improved long-term BGS measurement accuracy.

In conclusion, to improve the long-term measurement accuracy of PFGI-POF-based single-end-access Brillouin sensors, we have developed a new Fresnel suppression method using CYTOP dissolved in a volatile solvent. Through our experiments, we are able to confirm that Fresnel reflection can be permanently mitigated by covering the open end of the PFGI-POF with the CYTOP solution, even after solvent evaporation. Moreover, the high viscosity of CYTOP is advantageous compared to the conventional water-based method. If combined with angled-cut ends, this method would enhance the measurement accuracy further. Thus, we believe that this method can be adopted as a standard technique for improving the performance of PFGI-POF-based Brillouin sensing systems.

Acknowledgments This work was supported by JSPS KAKENHI Grant Numbers 17H04930 and 17J07226, and by research grants from the Japan Gas Association, the ESPEC Foundation for Global Environment Research and Technology, the Association for Disaster Prevention Research, the Fujikura Foundation, and the Japan Association for Chemical Innovation.

1) A. H. Hartog, *An Introduction to Distributed Optical Fibre Sensors* (CRC Press, Boca Raton, FL, 2017).
2) T. Kurashima, T. Horiguchi, H. Izumita, S. Furukawa, and Y. Koyamada, IEICE Trans. Commun. **E76-B**, 382 (1993).
3) Q. Li, J. Gan, Y. Wu, Z. Zhang, J. Li, and Z. Yang, IEEE Photonics Technol. Lett. **28**, 1493 (2016).
4) F. Wang, W. Zhan, X. Zhang, and Y. Lu, J. Lightwave Technol. **31**, 3663 (2013).
5) T. Horiguchi and M. Tateda, J. Lightwave Technol. **7**, 1170 (1989).
6) Y. Peled, A. Motil, and M. Tur, Opt. Express **20**, 8584 (2012).
7) Y. Muanenda, M. Taki, and F. D. Pasquale, Opt. Lett. **39**, 5411 (2014).
8) Y. Dong, D. Ba, T. Jiang, D. Zhou, H. Zhang, C. Zhu, Z. Lu, H. Li, L. Chen, and X. Bao, IEEE Photonics J. **5**, 2600407 (2013).
9) A. Minardo, R. Bernini, R. Ruiz-Lombera, J. Mirapeix, J. M. Lopez-Higuera, and L. Zeni, Opt. Express **24**, 29994 (2016).
10) D. Garus, K. Krebber, and F. Schliep, Opt. Lett. **21**, 1402 (1996).
11) R. Bernini, A. Minardo, and L. Zeni, IEEE Photonics J. **4**, 48 (2012).
12) K. Hotate and T. Hasegawa, IEICE Trans. Electron. **E83-C**, 405 (2000).
13) Y. H. Kim, K. Lee, and K. Y. Song, Opt. Express **23**, 33241 (2015).
14) W. Zou, C. Jin, and J. Chen, Appl. Phys. Express **5**, 082503 (2012).
15) R. Cohen, Y. London, Y. Antman, and A. Zadok, Opt. Express **22**, 12070 (2014).
16) A. Denisov, M. A. Soto, and L. Thévenaz, Light: Sci. Appl. **5**, e16074 (2016).
17) Y. Mizuno, W. Zou, Z. He, and K. Hotate, Opt. Express **16**, 12148 (2008).
18) Y. Mizuno, W. Zou, Z. He, and K. Hotate, J. Lightwave Technol. **28**, 3300 (2010).
19) Y. Mizuno and K. Nakamura, Appl. Phys. Lett. **97**, 021103 (2010).
20) Y. Dong, P. Xu, H. Zhang, Z. Lu, L. Chen, and X. Bao, Opt. Express **22**, 26510 (2014).
21) A. Minardo, R. Bernini, and L. Zeni, IEEE Photonics Technol. Lett. **26**, 387 (2014).
22) N. Hayashi, Y. Mizuno, and K. Nakamura, J. Lightwave Technol. **32**, 3999 (2014).
23) H. Lee, N. Hayashi, Y. Mizuno, and K. Nakamura, J. Lightwave Technol. **35**, 2306 (2017).
24) N. Hayashi, Y. Mizuno, and K. Nakamura, Opt. Express **20**, 21101 (2012).
25) I. R. Husdi, K. Nakamura, and S. Ueha, Meas. Sci. Technol. **15**, 1553 (2004).
26) K. Minakawa, N. Hayashi, Y. Mizuno, and K. Nakamura, IEEE Photonics Technol. Lett. **27**, 1394 (2015).
27) H. Lee, N. Hayashi, Y. Mizuno, and K. Nakamura, IEEE Photonics J. **8**, 6802807 (2016).
28) Y. Mizuno, N. Hayashi, H. Fukuda, K. Y. Song, and K. Nakamura, Light: Sci. Appl. **5**, e16184 (2016).
29) Y. Mizuno, N. Hayashi, H. Fukuda, and K. Nakamura, Jpn. J. Appl. Phys. **56**, 072501 (2017).
30) M. G. Kuzyk, *Polymer Fiber Optics: Materials, Physics, and Applications* (CRC Press, Boca Raton, FL, 2006).
31) Y. Koike and M. Asai, NPG Asia Mater. **1**, 22 (2009).
32) K. Minakawa, N. Hayashi, Y. Mizuno, and K. Nakamura, Appl. Phys. Express **6**, 052501 (2013).
33) Y. Akimoto, M. Asai, K. Koike, K. Makino, and Y. Koike, Opt. Lett. **37**, 1853 (2012).
34) Y. Mizuno, N. Hayashi, and K. Nakamura, J. Lightwave Technol. **32**, 4734 (2014).
35) M. Naritomi, H. Murofushi, and N. Nakashima, Bull. Chem. Soc. Jpn. **77**, 2121 (2004).
36) T. Ishigure, Y. Koike, and J. W. Fleming, J. Lightwave Technol. **18**, 178 (2000).
37) Y. Mizuno, N. Hayashi, and K. Nakamura, Electron. Lett. **50**, 1153 (2014).